PUBLICATIONS OF THE ASTRONOMICAL SOCIETY OF THE PACIFIC
97:1119-1126, November 1985

CALIBRATION OF THE LICK RED CCD BANDPASSES*

S. DJORGOVSKI

Astronomy Department, University of California, Berkeley, California 94720

Received 10 June 1985, revised 1985 July 12

Red bandpasses indigenous to the Lick Observatory CCD imaging and photometry are defined and described. A set of primary calibration standards which define the magnitude zero points is presented. Color equations relating these bandpasses to the other, commonly used photometric systems are evaluated by numerical integration of stellar spectra, and compared to the real data. It is estimated that the present calibration is accurate and consistent to about 2–3% as a magnitude predictor, if the primary standards are used; this accuracy is only about 3–5% if *VR* photometry is used for calibration, and only about 5–8% if *BV* photometry is used. (These estimates do not include the errors of measurement.) This is sufficient for most scientific applications of data taken in these bandpasses, although it may be improved somewhat in a future work.

Key word: photometry

I. Introduction and Motivation

Charge-coupled devices (CCDs) have been actively used at Lick Observatory for imaging and photometry since 1981. By far most of the data have been obtained in nonstandard, broad red bandpasses, defined below. These bandpasses are distinguished by the use of particular red filters, designed to avoid the prominent night-sky emission features. The filters were designed and purchased some years ago by H. Spinrad, and have been in active and productive use ever since. Two filters are used for direct imaging, one at the Shane 120-inch telescope, and one at the Nickel 40-inch telescope. Their transmission curves were originally identical, but they are not so any more, as the filters have aged differentially. They are probably fairly stable now, at least on the scale of a few years.

A number of papers in the literature cite the "red" magnitudes obtained with Lick CCD cameras and these filters. At least two large surface photometry surveys of galaxies (Lauer 1983, 1985*a*,*b*; Djorgovski and Davis 1983, and in preparation), and one survey of globular clusters (Djorgovski and Penner 1984, 1985, and in preparation) employ these bandpasses. Yet no satifactory color calibration for them has been produced until now. There is clearly a need to do so, as there is a large body of scientific data already obtained in these bandpasses, and more imaging and photometric data are produced almost daily at Lick.

The purpose of this paper is to define the color system of the Lick red CCD band-passes and relate it to the other commonly used photometric systems. This is not an attempt to achieve a high photometric accuracy. Rather, a few percent calibration is deemed adequate for the present purpose, since most applications of this color system (e.g., imaging of very faint objects, or relative surface photometry) do not require absolute calibration of the data any better than a few percent, and the systems are probably not stable in time to any better level of accuracy. This lack of stability is mainly due to continuous engineering changes and improvements in the Lick CCD systems. Finally, some relevant variables, such as the CCD quantum-efficiency curves are not well known, and may also change in time, e.g., due to new treatments, such as CCD backcharging. However, it is felt that these hardware changes do not afflict very significantly (e.g., more than say 1%) the color transformations explored here.

II. The Definition of the Bandpasses

The CCD systems at Lick Observatory are described by Robinson (1981), Lauer et al. (1983), and Miller (1983).

There are three distinct bandpasses, which we will designate as r_S, r_G, and r_T. Their effective wavelength response curves are shown in Figure 1, along with some other common red bandpasses.

The r_S bandpass is defined as a product of the quantum efficiency of a TI 3-phase 800 × 800 CCD, two reflections from aluminum, collimator, and camera lenses of the Cassegrain CCD system, and the Spinrad red filter at the 120-inch (3-m) telescope.

The r_G bandpass is defined as a product of the quantum efficiency of a GEC P8600 385 × 576 CCD, three reflections from aluminum, and the Spinrad red filter at the 40-inch (1-m) telescope. On some occasions, a Nikon speed-up lens was used with this system; its transmission is almost gray in the wavelength region of interest, and it does not modify the r_G bandpass appreciably.

The r_T bandpass is defined as a product of the quantum efficiency of a TI thinned 500 × 500 CCD, four reflections from aluminum, transmission of a Cannon speed-up lens, and the Spinrad red filter at the 40-inch telescope.

In order to produce the curves shown in Figure 1, we

*Based in part on the research done at Lick Observatory, University of California.

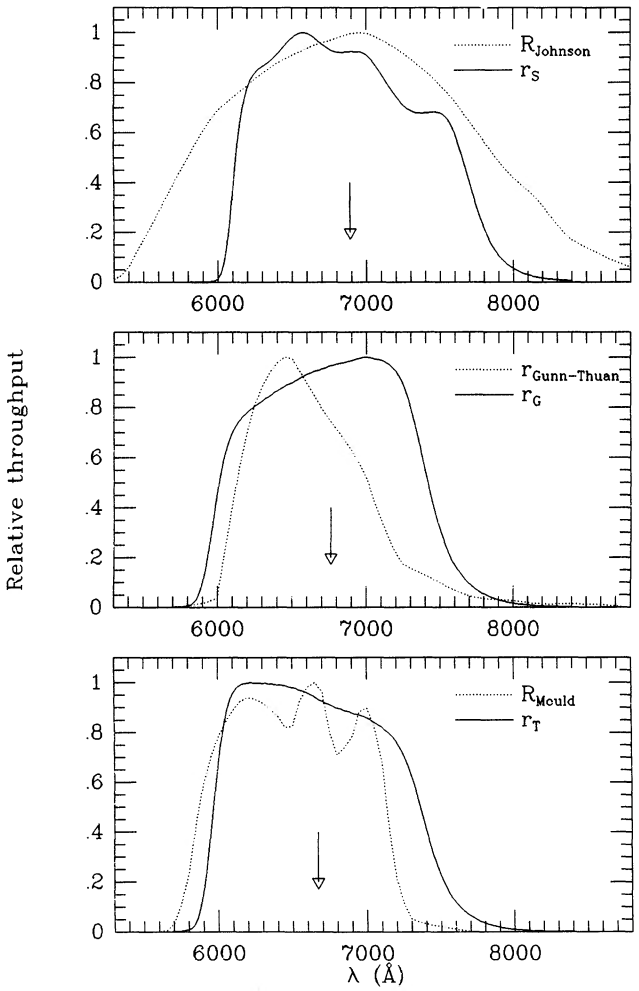

FIG. 1–Relative throughput curves for the Lick red CCD bandpasses (solid lines). Some other commonly used red bandpasses are shown for comparison. The arrows mark the effective wavelengths.

used the "typical" quantum efficiency curves for the CCD chips, as supplied by their respective manufacturers. These should be fairly accurate representations of the CCD's response, at least in shape of the curves, and at the red wavelengths, which are of interest here. Lens transmission tracings were supplied by Lick Observatory. Transmissions of the filters were measured directly with the 120-inch telescope spectrograph. Standard aluminum reflection curves were used. No transmission tracing for the Cannon lens of the r_T bandpass was available, so that the Nikon lens transmission curve was substituted for it. Note that only the shapes of these response curves are of interest, as the zero-points must be tied to the magnitude of α Lyrae.

Let us define the effective wavelength of a bandpass (following King 1952)

$$\lambda_{\rm eff} = \frac{\int \lambda T(\lambda) d\lambda}{\int T(\lambda) d\lambda} \qquad (1)$$

and the equivalent width of a bandpass as

$$W_\lambda = \frac{1}{T_{\rm max}} \int T(\lambda) d\lambda \quad , \qquad (2)$$

where $T(\lambda)$ is the bandpass response, and $T_{\rm max}$ its peak value, and the integration is carried over the whole bandpass. The effective wavelengths for the r_S, r_G, and r_T bandpasses are 6890Å, 6760Å, and 6670Å, and equivalent widths 1370Å, 1340Å, and 1340Å, respectively. For comparison, the Johnson R has $\lambda_{\rm eff}$ = 6940Å and $W\lambda$ = 2060Å.

Using the Vega calibration of Hayes and Latham (1975), we derive the following conversion into physically meaningful units at the effective wavelengths quoted above:

$r_S = 0$ corresponds to 2810 Jy ,
$r_G = 0$ corresponds to 2890 Jy ,
$r_T = 0$ corresponds to 2920 Jy .

Note that these conversions will be weak functions of color; they are given here for a neutral color object (viz., Vega, an A0V star).

Assuming these effective wavelengths, and using the interpolation tables of Seaton (1979), we obtain for Galactic extinction in these bandpasses:

$$A(r_G) = 0.75\, A_V = 2.40\, E_{B-V} \quad , \qquad (3)$$
$$A(r_T) = 0.76\, A_V = 2.44\, E_{B-V} \quad , \qquad (4)$$
$$A(r_S) = 0.73\, A_V = 2.34\, E_{B-V} \quad . \qquad (5)$$

In order to define the zero points for magnitudes in these bandpasses, fluxes of the spectroscopic standard stars of Stone (1974, 1977), Oke (1974), Philip and Hayes (1983), and Oke and Gunn (1983) were numerically integrated within the bandpass curves (as shown in Fig. 1). The flux of Vega, as given by Hayes and Latham (1975) was integrated in the same way, and used to determine the zero points for the system. The magnitudes of the flux standards are listed in Table I. They constitute the primary standards for this bandpass system. Absolute flux calibrations of these stars are uncertain by about 2% (according to the source papers), and the numerical errors of integrations are much smaller than that. The differences between the shapes of the theoretical bandpasses (as shown in Fig. 1) and the "true" bandpasses are not likely to be very important for the determination of the magnitude zero points, since most of the flux standards have very similar spectra in the red. Thus, the estimated errors of magnitudes for these primary standards is about 0.02–0.03 mag, and derive primarily from the uncertainty of their original F_ν measurements.

III. The Color Equations

Color transformations are necessary in order to relate these "red" magnitudes to other, commonly used systems, and in order to use the secondary photometric

TABLE I

Primary Flux Standards for the System

Star	rS	rG	rT
BD +08 2015	9.95	10.00	10.02
BD +25 3941	9.91	9.97	10.00
BD +26 2606	9.32	9.36	9.38
BD +28 4211	10.71	10.72	10.71
BD +33 2642	10.93	10.93	10.93
BD +40 4032	10.22	10.25	10.26
Feige 15	10.38	10.39	10.40
Feige 24	12.27	12.31	12.32
Feige 25	12.00	12.01	12.01
Feige 34	11.43	11.43	11.42
Feige 56	11.16	11.17	11.16
Feige 92	11.69	11.70	11.69
Feige 98	11.84	11.85	11.85
Feige 110	12.02	12.02	12.01
HD 37129	7.24	7.24	7.23
HD 86986	7.74	7.76	7.77
HD 109995	7.56	7.57	7.57
HD 161817	6.86	6.88	6.89
G 191 b2b	12.02	12.01	12.00
G 9937	14.14	14.17	14.19
Hiltner 102	9.81	9.87	9.91
Hiltner 600	10.29	10.31	10.32
HZ 15	12.58	12.60	12.60
HZ 534	7.52	7.54	7.56
Kopff 27	10.14	10.17	10.18
EG 129 (GrW)	13.16	13.18	13.18
Vega	0.025	0.025	0.025

Estimated errors are ~ 0.02 mag.

standards (typically available in the Johnson *UBVRI* system) for data calibrations.

The author has observed on numerous occasions the *UBVRI* standards of Landolt (1973, 1983), Christian et al. (1985), and others, as well as some of the Thuan-Gunn (1976) and Kent (1985) *uvgriz* system standards, and the primary spectrophotometric flux standards mentioned above. This was done mainly during the observing for surface photometry surveys, and the standard stars were not observed and processed for a high photometric accuracy. Moreover, the observing conditions were not always photometric, and the atmospheric extinction coefficients were not followed very closely. Although those calibration measurements were adequate for their purpose (approximate survey calibration), they are not always up to the standards of measurement necessary for a fiducial establishment of a photometric system.

It was felt that a better strategy for the homogeneous and consistent definition of diverse color equations is a numerical evaluation of all relations of interest, and subsequent comparison with better subsets of the real stellar data. This is in principle similar to the works of Buser (1978*a*,*b*) and Bell (1972*a*,*b*), who demonstrated usefulness of the method. A library of stellar spectra, compiled by Gustavo Bruzual for his modeling of galaxy evolution (Bruzual 1981, 1983), was used as a "data" set. Bandpass curves for the standard Johnson-Morgan *UBVRI* system were used, along with the curves for the Bessell (1976) and Mould (KPNO CCD) versions (the latter were published by Butcher and Jacoby 1983). The curves for the Gunn-Thuan *uvgriz* system were taken from Schneider (1982). Also used were the photographic *JF* bandpasses, as given by Bruzual (1981), and the CCD *JF* bandpasses from Schild and Kent (1981). All stellar spectra were converted into photon count per unit wavelength, and integrated in all the bandpasses. The zero points were set by demanding that an A0V star has a zero color in all bands, except for the *uvgriz* system, whose zero points were determined from its primary standards BD +28°4211 and Feige 34. Low-order polynomials were then fitted to these synthetic colors.

Listed below are some of the color equations, typically broken at the "Johnson knee" into two linear relations; in some cases, a single quadratic relation was more appropriate. Listed in the square brackets are the standard deviations of the scatter around these equations. These "theoretical" errors are indicative of the quality of the least-squares fit *only*: the "true" errors of these color transformations are likely to be slightly higher, since the exact forms of the bandpass response curves is not extremely well known. In addition, in any realistic situation, the quoted magnitude and color errors of the calibration standards used (typically 0.005 to 0.03 mag) *and* the user's measurement errors should be added to these figures. In the case of the r_S bandpass, the red tail of the response curve is not well known, and there is a possibility of an unaccounted red leak in the present computation of the color equations. Some examples of the color equations and their least-squares fits are shown graphically in Figure 2. Many other relations were determined but are not listed here as they are of limited interest. They are available from the author on request.

Mutual relations of the r_G, r_T, and r_S bands, as functions of the Johnson *BVR* colors are:

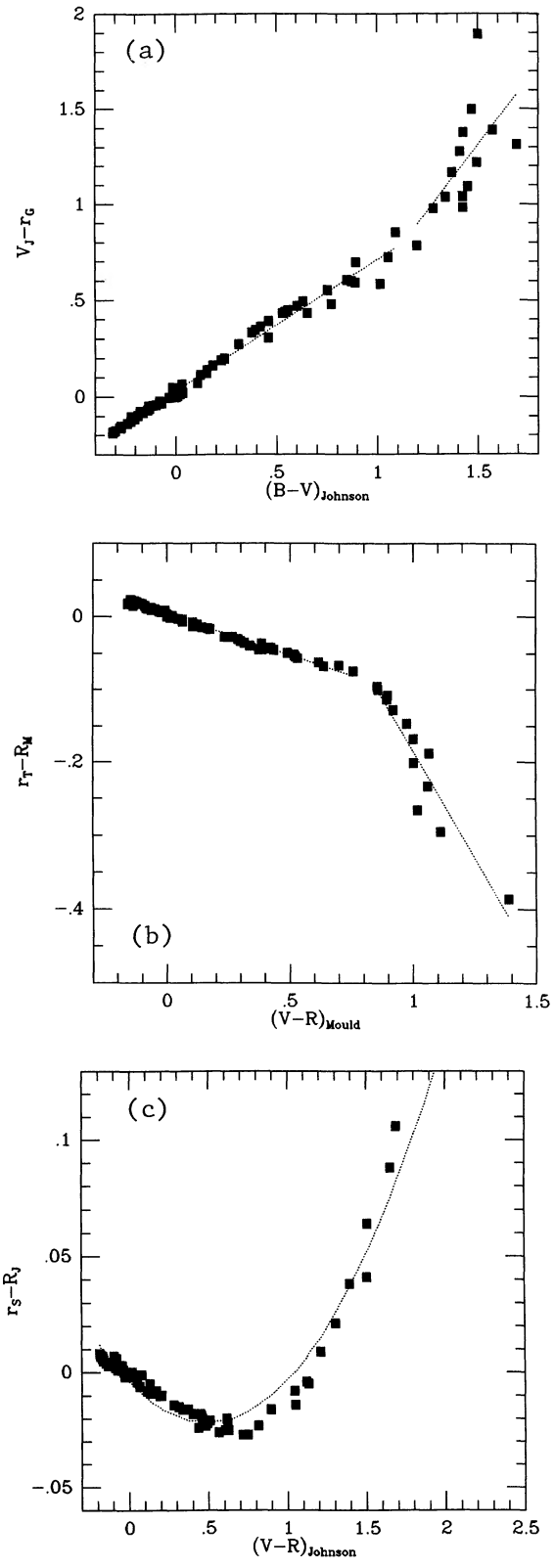

FIG. 2–Some examples of the numerically derived color equations. The points correspond to different spectral types, and the dotted lines represent the least-squares fits to them. The three panels correspond to (a) equation (12) (b) equation (22), and (c) equation (17) (see the text).

$$(r_G - r_T) = 0.000 - 0.036(B-V)_J\,[0.002] \text{ for } (B-V)_J < 1.25 \quad (6a)$$
$$(r_G - r_T) = 0.143 - 0.159(B-V)_J\,[0.029] \text{ for } (B-V)_J > 1.25 \quad (6b)$$
$$(r_G - r_T) = 0.001 - 0.052(V-R)_J\,[0.001] \text{ for } (V-R)_J < 1.0 \quad (7a)$$
$$(r_G - r_T) = 0.036 - 0.086(V-R)_J\,[0.004] \text{ for } (V-R)_J > 1.0 \quad (7b)$$
$$(r_G - r_S) = 0.002 + 0.049(B-V)_J\,[0.003] \text{ for } (B-V)_J < 1.25 \quad (8a)$$
$$(r_G - r_S) = -0.249 + 0.270(B-V)_J\,[0.050] \text{ for } (B-V)_J > 1.25 \quad (8b)$$
$$(r_G - r_S) = 0.000 + 0.070(V-R)_J\,[0.002] \text{ for } (V-R)_J < 1.0 \quad (9a)$$
$$(r_G - r_S) = -0.065 + 0.144(V-R)_J\,[0.013] \text{ for } (V-R)_J > 1.0 \quad (9b)$$
$$(r_S - r_T) = -0.003 - 0.085(B-V)_J\,[0.005] \text{ for } (B-V)_J < 1.25 \quad (10a)$$
$$(r_S - r_T) = 0.392 - 0.430(B-V)_J\,[0.079] \text{ for } (B-V)_J > 1.25 \quad (10b)$$
$$(r_S - r_T) = 0.001 - 0.122(V-R)_J\,[0.003] \text{ for } (V-R)_J < 1.0 \quad (11a)$$
$$(r_S - r_T) = 0.102 - 0.230(V-R)_J\,[0.018] \text{ for } (V-R)_J > 1.0 \quad (11b)$$

The $(B-V)$ color index is used here mainly as a variable measuring the spectral type.

Transformations into the Johnson *BVR* system are:

$$(V_J - r_G) = 0.031 + 0.681(B-V)_J\,[0.032] \text{ for } (B-V)_J < 1.1 \quad (12a)$$
$$(V_J - r_G) = -0.768 + 1.386(B-V)_J\,[0.228] \text{ for } (B-V)_J > 1.1 \quad (12b)$$
$$(V_J - r_T) = 0.030 + 0.638(B-V)_J\,[0.029] \text{ for } (B-V)_J < 1.05 \quad (13a)$$
$$(V_J - r_T) = -0.495 + 1.138(B-V)_J\,[0.187] \text{ for } (B-V)_J > 1.05 \quad (13b)$$
$$(V_J - r_S) = 0.033 + 0.740(B-V)_J\,[0.028] \text{ for } (B-V)_J < 1.0 \quad (14a)$$
$$(V_J - r_S) = -0.929 + 1.596(B-V)_J\,[0.246] \text{ for } (B-V)_J > 1.0 \quad (14b)$$
$$(r_G - R_J) = -0.001 + 0.034(V-R)_J\,[0.003] \text{ for } (V-R)_J < 1.0 \quad (15a)$$
$$(r_G - R_J) = -0.306 + 0.350(V-R)_J\,[0.013] \text{ for } (V-R)_J > 1.0 \quad (15b)$$
$$(r_T - R_J) = -0.002 + 0.086(V-R)_J\,[0.003] \text{ for } (V-R)_J < 1.0 \quad (16a)$$
$$(r_T - R_J) = -0.303 + 0.406(V-R)_J\,[0.025] \text{ for } (V-R)_J > 1.0 \quad (16b)$$
$$(r_S - R_J) = -0.004 - 0.072(V-R)_J + 0.073\,(V-R)_J^2\,[0.008] \quad (17)$$

The color equations involving the $(B-V)$ color indices do not work as well as the equations involving the $(V-R)$ color index, as it may be expected for these red magnitudes. This is indeed verifed by the comparisons with the real data in Section IV below. However, in some cases only the *UBV* photometry, and no *VRI* photometry is available, and the equations (12)–(14) become useful.

Transformations into the Bessell (1976, 1979) *VR* system are:

$$(r_G - R_B) = -0.001 - 0.507(V-R)_B + 0.203(V-R)_B^2\,[0.006] \quad (18)$$
$$(r_T - R_B) = -0.003 - 0.430(V-R)_B + 0.229(V-R)_B^2\,[0.008] \quad (19)$$
$$(r_S - R_B) = 0.000 - 0.514(V-R)_B\,[0.013] \text{ for} (V-R)_B < 1.0 \quad (20a)$$
$$(r_S - R_B) = -0.318 - 0.168(V-R)_B\,[0.008] \text{ for} (V-R)_B > 1.0 \quad (20b)$$

Please note that Bessell (1979) gives transformations of his system into the Kron and Cousins systems.

Transformations into the Mould KPNO CCD VR system are:

$$(r_G - R_M) = 0.005 - 0.173(V-R)_M\,[0.005] \text{ for } (V-R)_M < 0.8 \quad (21a)$$
$$(r_G - R_M) = 0.526 - 0.798(V-R)_M\,[0.043] \text{ for } (V-R)_M > 0.8 \quad (21b)$$
$$(r_T - R_M) = 0.003 - 0.111(V-R)_M\,[0.003] \text{ for } (V-R)_M < 0.8 \quad (22a)$$
$$(r_T - R_M) = 0.399 - 0.583(V-R)_M\,[0.031] \text{ for } (V-R)_M > 0.8 \quad (22b)$$
$$(r_S - R_M) = 0.005 - 0.257(V-R)_M\,[0.006] \text{ for } (V-R)_M < 0.8 \quad (23a)$$
$$(r_S - R_M) = 0.734 - 1.148(V-R)_M\,[0.068] \text{ for } (V-R)_M > 0.8 \quad (23b)$$

Transformations into the Gunn-Thuan CCD *gr* system are:

$$(r_G - r) = -0.305 - 0.045(g-r)\,[0.003] \text{ for } (g-r) < 0.7 \quad (24a)$$
$$(r_G - r) = -0.175 - 0.241(g-r)\,[0.017] \text{ for } (g-r) > 0.7 \quad (24b)$$
$$(r_T - r) = -0.283 - 0.002(g-r)\,[0.002] \text{ for } (g-r) < 0.7 \quad (25a)$$
$$(r_T - r) = -0.205 - 0.109(g-r)\,[0.009] \text{ for } (g-r) > 0.7 \quad (25b)$$
$$(r_S - r) = -0.339 - 0.104(g-r)\,[0.005] \text{ for } (g-r) < 0.7 \quad (26a)$$
$$(r_S - r) = -0.132 - 0.451(g-r)\,[0.041] \text{ for } (g-r) > 0.7 \quad (26b)$$

However, the *gr* magnitude zero points (as determined from the primary standards of this system) are uncertain by about 0.02 mag, and that error should be added to the transformation errors quoted above, where appropriate.

Transformations into the photographic *JF* system are:

$$(r_G - F_{pg}) = -0.013 - 0.260(J-F)_{pg}\,[0.003] \text{ for } (J-F)_{pg} < 1.5 \quad (27a)$$
$$(r_G - F_{pg}) = \;\;0.931 - 0.842(J-F)_{pg}\,[0.059] \text{ for } (J-F)_{pg} > 1.5 \quad (27b)$$
$$(r_T - F_{pg}) = -0.012 - 0.227(J-F)_{pg}\,[0.012] \text{ for } (J-F)_{pg} < 1.7 \quad (28a)$$
$$(r_T - F_{pg}) = \;\;0.605 - 0.613(J-F)_{pg}\,[0.053] \text{ for } (J-F)_{pg} > 1.7 \quad (28b)$$
$$(r_S - F_{pg}) = -0.016 - 0.302(J-F)_{pg}\,[0.015] \text{ for } (J-F)_{pg} < 1.7 \quad (29a)$$
$$(r_S - F_{pg}) = 1.090 - 1.024(J-F)_{pg}\,[0.100] \text{ for } (J-F)_{pg} > 1.7 \quad . \quad (29b)$$

Transformations into the Schild-Kent CCD *JF* system are:

$$(r_G - F_{CCD}) = -0.002 - 0.042(J-F)_{CCD}\,[0.003] \text{ for } (J-F)_{CCD} < 1.5 \quad (30a)$$
$$(r_G - F_{CCD}) = -0.007 + 0.003(J-F)_{CCD}\,[0.008] \text{ for } (J-F)_{CCD} > 1.5 \quad (30b)$$
$$(r_T - F_{CCD}) = -0.001 - 0.015(J-F)_{CCD}\,[0.002] \text{ for } (J-F)_{CCD} < 1.6 \quad (31a)$$
$$(r_T - F_{CCD}) = -0.227 + 0.116(J-F)_{CCD}\,[0.013] \text{ for } (J-F)_{CCD} > 1.6 \quad (31b)$$
$$(r_S - F_{CCD}) = -0.004 - 0.077(J-F)_{CCD}\,[0.004] \text{ for } (J-F)_{CCD} < 1.7 \quad (32a)$$
$$(r_S - F_{CCD}) = -0.145 - 0.162(J-F)_{CCD}\,[0.016] \text{ for } (J-F)_{CCD} > 1.7 \quad . \quad (32b)$$

The numerical procedure used to evaluate these color equations can be tested by comparing the predicted r_G, r_T, or r_S magnitude from different relations, e.g., from the flux standards (Table I) which are also the *uvgriz* primary standards (Kent 1985); the discrepancies are indeed within the quoted error bars. However, the true test is the comparison with real data of reasonably good photometric quality, as shown below.

IV. Comparison with the Direct Measurements

The color equations developed in the previous section can be used as r_G, r_T, or r_S magnitude predictors for the photometric standards for which a good photometry is available in one of the systems explored above.

Stellar photometry, obtained for the calibration of a surface photometry survey (Djorgovski and Davis 1983, and in preparation) was processed in this manner. The observations were done at the Lick 40-inch telescope, in r_G and r_T bandpasses. The instrumental stellar magnitudes were measured in fixed circular apertures, with typical radii of the order of 5 to 7 arc sec (depending on the seeing for a given night). The sky foreground was determined and subtracted locally. No extinction coefficients were followed during the night; instead, the air mass at each pointing was computed, and a standard atmospheric extinction for the appropriate effective wavelength was derived, and the data corrected for it. Thus, the photometry is only of a medium quality at its best, but it is the only such data set available at the moment. The estimated errors for the instrumental magnitudes are typically of the order of 0.03 to 0.06 mag, although they may be worse in some cases. Poissonian noise of the detector and the extinction uncertainties are approximately equal contributors to these errors. This estimate was made both through the direct computation of the number of electrons, and the comparisons of instrumental magnitudes of stars for which multiple exposures were available.

The following photometric standards were observed: selected Landolt (1973, 1983) Johnson system *UBVRI* standards, some *RI* magnitudes for some of which were taken from Moffett and Barnes (1979); Christian et al. (1985) standard fields, with their *UBVRI* measurements converted into the Johnson system; M 67 *UBV* measurements of Johnson and Sandage (1955) and Eggen and Sandage (1964), supplemented by some *RI* measurements of Mendoza (1967); Thuan and Gunn (1976) and Kent (1985) *uvgriz* system standards; and many of the flux standards listed in Table I. The r_G or r_T magnitudes were derived from the source data and the appropriate color transformations, listed in the previous section. For the flux standards, the magnitudes given in Table I were used.

For each night and each star, the difference between the instrumental and the predicted magnitude (r_G or r_T) was computed, and the weighted average of the mean and median differences was adopted as the magnitude zero point (m_0) for the night. This quantity was then subtracted from the original magnitude differences, and the deviations thus obtained are shown in Figures 3–8. Only the estimated error bars from the color transformations (which also include the estimated errors of the source magnitudes) are shown. The rest of the scatter is completely explainable by the measurement error bars, which are typically a few percent. As it may be expected, the *VR* data have considerably less scatter than the *BV* data as estimators for these red magnitudes. The *gr* photometry also works very well. In the case of r_S photometry, the data indicate a possible (but statistically not very significant) residual slope; this may be an indication of an unknown red leak. Some simple comparisons of flux standards taken on the same night indicate that the r_S magnitudes defined by Table I are certainly good to about 2% or 3%, plus the measurement errors.

It thus appears that the proposed calibration for this bandpass system is accurate and self-consistent to a level of a few percent, which is no worse than the typical measuring errors in most applications. The best results (2%–3% accuracy, plus the measurement errors) can be achieved if the primary flux standards (listed in TableI) are used. Lacking that, *VR* photometric standards should provide a calibration accurate to about 5%, or better, plus the measurement errors. As a last resort, *BV* photometric

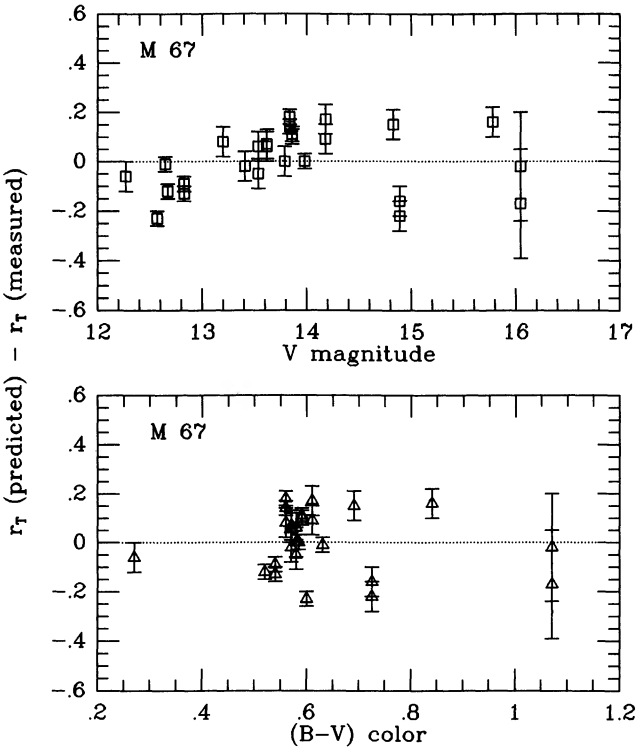

FIG. 3–Comparison of the predicted and the measured r_T magnitudes as a function of the V magnitude (top) or $(B-V)$ color index (bottom). The M67 data were obtained on 1982 April 23 UT, in moderately good photometric conditions. The error bars do not include the measurement errors of instrumental magnitudes, which account for the residual scatter. They include only the errors of the source magnitudes and the color transformations. Equation (13) was used as the r_T predictor.

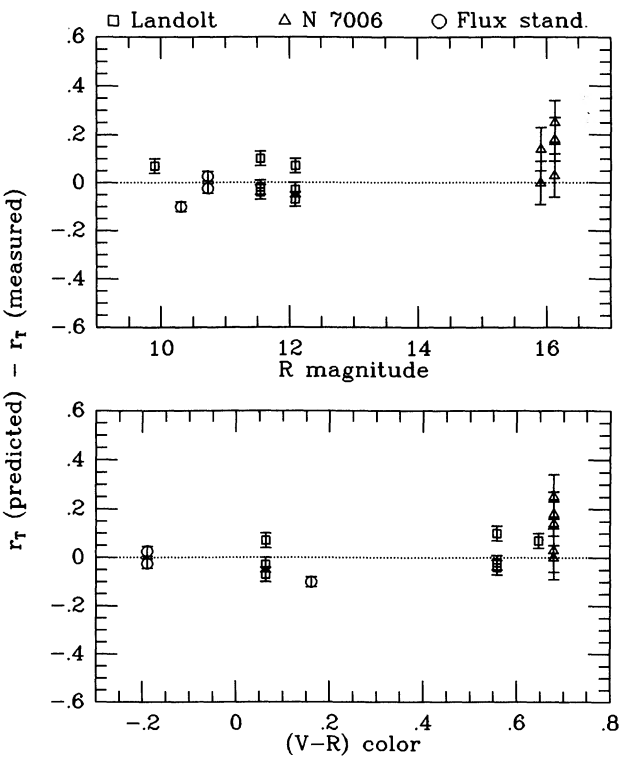

FIG. 4–Comparison of the predicted and the measured r_T magnitudes as a function of the R magnitude (top) or $(V-R)$ color index (bottom). The data were obtained on 1982 October 15 and 18 UT, in fairly good photometric conditions. The error bars do not include the measurement errors of instrumental magnitudes, which account for the residual scatter. They include only the errors of the source magnitudes and the color transformations. Equation (16) was used as the r_T predictor.

standards should provide a calibration accurate to about 5%–10% only, plus the measurement errors. The situation can be improved considerably with a devoted effort to specifically measure the magnitudes of standard stars in good photometric conditions, and more sophisticated data-reduction methods. That, however, is beyond the scope of the present paper.

I am very grateful to the staff of Lick Observatory for their continuous help with the equipment and observations. CCD quantum efficiency curves were communicated by J. Miller and L. Robinson, and the lens transmission curves by R. Stover. Hy Spinrad invented the filters and helped in measurement of their transmission curves. Data used to construct Figure 8 were obtained by S. Kulkarni and P. McCarthy. Some of the software used for this work was developed by T. Lauer, R. Stover, and D. Terndrup. Marc Davis provided support, occasional help, and much needed prodding. Ivan King provided indoctrination on magnitudes and much good advice. I acknowledge helpful criticism of an anonymous referee. This work was partly supported by NSF grant AST 81-18557, and a University of California Regents fellowship.

REFERENCES

Bell, R. A. 1972*a*, *M.N.R.A.S.* **159**, 349.
Bell, R. A. 1972*b*, *M.N.R.A.S.* **159**, 357.
Bessel, M. S. 1976, *Pub. A.S.P.* **88**, 557.
Bessel, M. S. 1979, *Pub. A.S.P.* **91**, 589.
Bruzual, G. 1981, Ph. D. Thesis, University of California at Berkeley.
Bruzual, G. 1983, *Ap. J.* **273**, 105.
Buser, R. 1978*a*, *Astr. and Ap.* **62**, 411.
Buser, R. 1978*b*, *Astr. and Ap.* **62**, 425.
Butcher, H., and Jacoby, G. 1983, *KPNO Newsletter* No. 25, 11.
Christian, C. A., Adams, M. A., Barnes, J. V., Butcher, H., Hayes, D. S., Mould, J. M., and Siegel, M. 1985, *A.S.P.* **97**, 363.
Djorgovski, S., and Davis, M. 1983, *Bull. A.A.S.* **15**, 932.
Djorgovski, S., and Penner, H. 1984, *Bull. A.A.S.* **16**, 501.
Djorgovski, S., and Penner, H. 1985, in *The Dynamics of Star Clusters, I.A.U. Symposium No. 113*, P. Hut and J. Goodman, eds. (Boston: Reidel), p. 73.
Eggen, O. J., and Sandage, A. R. 1964, *Ap. J.* **140**, 130.
Johnson, H. J., and Sandage, A. R. 1955, *Ap. J.* **121**, 616.
Hayes, D. S., and Latham, D. W. 1975, *Ap. J.* **197**, 593.
Kent, S. M. 1985, *Pub. A.S.P.* **97**, 165.
King, I. R. 1952, *Ap. J.* **115**, 580.
Landolt, A. U. 1973, *A.J.* **78**, 959.
Landolt, A. U. 1983, *A.J.* **88**, 439.
Lauer, T. R. 1983, Ph. D. Thesis, University of California at Santa Cruz.
Lauer, T. R. 1983*a*, Ap. J. Suppl. **57**, 473.
Lauer, T. R. 1985*b*, *Ap. J.* **292**, 104.

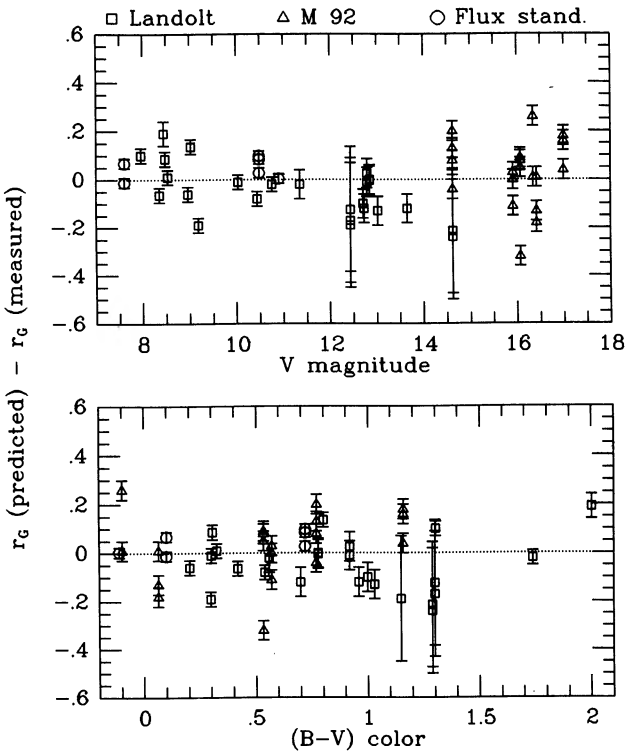

FIG. 5–Similar to Figure 3, but for the r_G magnitudes. The data were obtained on 1983 May 16 through 20 UT, in variable photometric conditions. The meaning of the error-bars is the same as in Figures 3 and 4. Equation (12) was used as the r_G predictor.

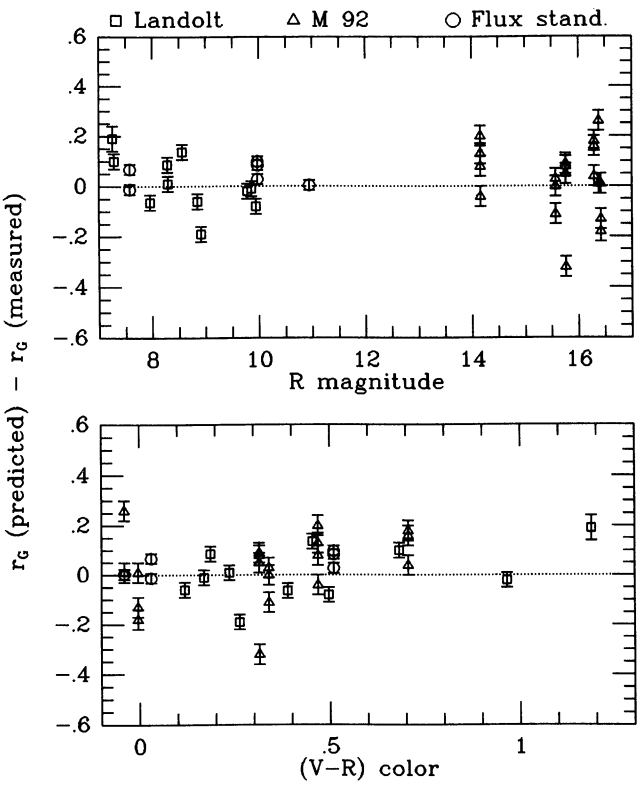

FIG. 6–Similar to Figure 4, but for the r_G magnitudes. The data were obtained on 1983 May 16 through 20 UT, in variable photometric conditions. The meaning of the error-bars is the same as in Figures 3, 4, and 5. Equation (15) was used as the r_G predictor.

Lauer, T. R., Miller, J. S., Osborne, C. S., Robinson, L. B., and Stover, R. J. 1983, *Proc. S.P.I.E.* **445**, 132.
Mendoza, E. E. 1967, *Bol. Obs. Tonantzitla y Tacubaya* **4**, 149.
Miller, J. S. 1983, Lick Observatory internal report.
Moffett, T. J., and Barnes, T. G. 1979, *A.J.* **84**, 627.
Oke, J. B. 1974, *Ap. J. Suppl.* **27**, 21.
Oke, J. B., and Gunn, J. E. 1983, *Ap. J.* **266**, 713.
Philip, A. G. D., and Hayes, D. S. 1983, *Ap. J. Suppl.* **53**, 751.
Robinson, L. B. 1981, *Proc. S.P.I.E.* **290**, 124.
Schild, R., and Kent, S. 1981, *Proc. S.P.I.E.* **290**, 186.
Schneider, D. 1982, Ph. D. Thesis, California Institute of Technology.
Seaton, M. J. 1979, *M.N.R.A.S.* **187**, 73p.
Stone, R. P. S. 1974, *Ap. J.* **193**, 135.
Stone, R. P. S. 1977, *Ap. J.* **218**, 767.
Thuan, T. X., and Gunn, J. E. 1976, *Pub. A.S.P.* **88**, 543.

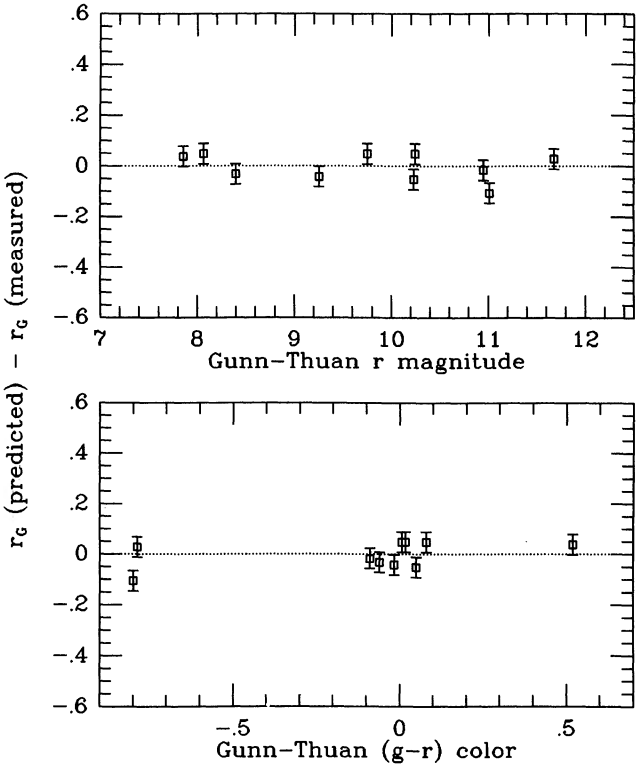

FIG. 7–Comparison of the measured r_G magnitudes with the magnitudes predicted from equation (24), using the Gunn-Thuan *gr* primary standards. Several of those stars were observed during the May 1983, September 1983, January 1984, and March 1984 runs, in variable (mostly good) photometric conditions. The meaning of the error bars is the same as in Figures 3, 4, 5, and 6.

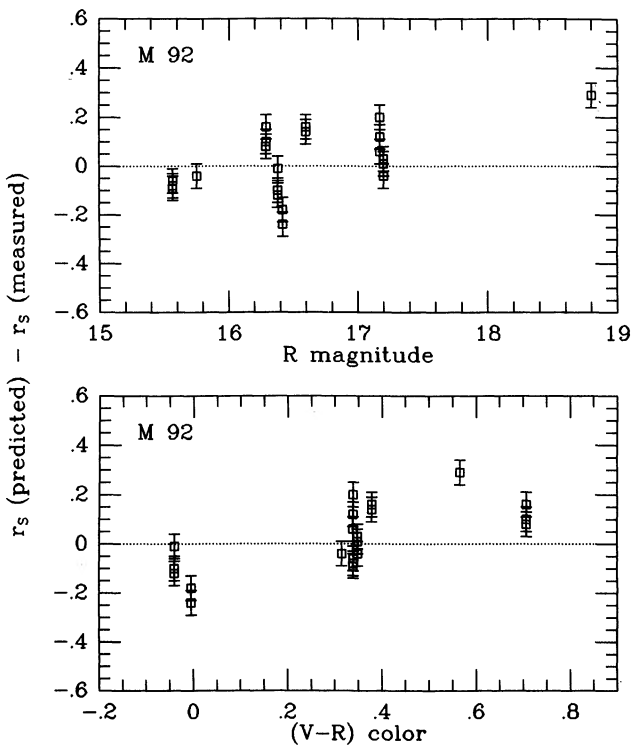

FIG. 8–Similar to Figure 4, but for the r_S magnitudes. The data on M92 KPNO standards of Christian et al. (1985) were obtained on 1985 June 18 UT, in fair photometric conditions. The meaning of the error bars is the same as in Figures 3, 4, and 5. Equation (17) was used as the r_S predictor. Possible residual slopes may be due to a poorly-known red leak.